

1 Epidemic dynamics shape inferences of the differences in
2 incubation-period and generation-interval distributions of the
3 Delta and Omicron variants
4

5 **Abstract**

6 Estimating the differences in the incubation-period and serial-interval distributions
7 of SARS-CoV-2 variants is critical to understanding changes in their transmission
8 dynamics and therefore controlling their outbreaks. However, these comparisons
9 are inherently difficult due to their dependence on epidemic growth rates—for
10 example, when an epidemic is growing exponentially, we are more likely to observe
11 individuals who have been infected recently, decreasing the mean observed
12 incubation period and thereby increasing the mean observed serial interval. Here,
13 we analyze serial-interval data describing transmissions of the Delta and Omicron
14 variants from Netherlands at the end of December 2021, during which the number
15 of infections caused by the Delta variant decreased as the number of Omicron
16 infections increased. Accounting for growth-rate differences of two variants, we
17 estimate similar mean incubation periods (3.8–4.5 days) for both variants but a
18 shorter mean generation interval for the Omicron variant (3.3 days; 95% CI: 2.8–3.7
19 days) than for the Delta variant (4.2 days; 95% CI: 4.0–4.4 days). These differences
20 may reflect higher reproduction numbers of the Omicron variant, which can drive
21 faster susceptible depletion among close contacts. Neglecting differences in the
22 generation-interval distributions can further bias in estimates of transmission
23 advantages of the Omicron variant.

1 Introduction

Estimating transmission advantages of new SARS-CoV-2 variants is critical to predicting and controlling the course of the ongoing COVID-19 pandemic. Transmission advantages of invading variants are typically characterized by the ratios of reproduction numbers, $\mathcal{R}_{\text{inv}}/\mathcal{R}_{\text{res}}$, and the differences in growth rates, $r_{\text{inv}} - r_{\text{res}}$. These two quantities are linked by the generation-interval distributions of the resident and invading variants. For example, an invading variant with shorter generation intervals—defined as the time between infection of the infector and the infectee—will exhibit faster epidemic growth ($r_{\text{inv}} > r_{\text{res}} > 0$) even if their reproduction numbers are identical ($\mathcal{R}_{\text{inv}} = \mathcal{R}_{\text{res}} > 1$).

Estimating generation-interval is hard, largely due to difficulties in observing actual infection events. Many researchers primarily focus on comparisons of other transmission intervals, such as time between symptom onsets (also referred to as serial intervals) or between testing events [1] of the infector and the infectee. However, transmission-interval distributions are subject to dynamical effects which can bias estimation. For example, when the epidemic is growing, a cohort of infectors who developed symptoms at the same time are more likely to have been infected recently, shortening their incubation periods—in other words, their incubation periods will be shorter, on average, than those of their infectees, causing the mean serial interval to be longer than the mean generation interval [2]. Therefore, observed differences in transmission-interval distributions between variants can give a biased picture of true differences in their generation-interval distributions, especially if their growth rates differ.

Here, we re-analyze serial-interval data collected by [3], representing within- and between-household transmissions of the Delta and Omicron variants from the Netherlands between 13 and 26 December 2021. The authors of the original article reported shorter serial intervals (3.5 vs 4.1 days) and incubation periods (3.2 vs 4.4 days) for transmission pairs with S-gene target failure (mostly omicron during the study period) and without (mostly delta), but did not consider growth-rate differences in their inference. Here, we discuss the epidemiological context in the Netherlands during the study period and take dynamics into account to provide corrected estimates for the incubation periods and generation-interval distributions of the Delta and Omicron variants.

2 Methods

2.1 Data

We analyze time series of reported COVID-19 cases (<https://data.rivm.nl/covid-19/>) and proportions of SARS-CoV-2 variants detected (<https://www.rivm.nl/coronavirus-covid-19/virus/varianten>) from the Netherlands between 29 November 2021 and 30 January 2022. Both data are publicly available on the National Institute for Public Health

63 and the Environment (RIVM) website.

64 Serial interval data are taken from the supplementary material of [3]. The data are
65 aggregated by the length of the serial interval in days and do not include additional
66 individual-level information, such as exposure dates or symptom onset dates. The
67 data consists of 2529 transmission pairs and are further stratified by the presence of
68 S gene target failure, week of infectors' symptom onset date (week 50 and 51), and
69 the type of transmission (within or between households). For simplicity, we refer
70 to transmission pairs with and without S gene target failure as Omicron and Delta
71 transmission pairs, respectively. See original article for details of data collection.

72 **2.2 Estimating epidemic growth rates**

73 To estimate the differences in growth rates of the Delta and Omicron variants, we
74 first estimate the number of COVID-19 cases caused by each variant by multiplying
75 reported weekly numbers of cases by the proportion of Delta and Omicron variants
76 detected—we use weekly time series to smooth over patterns of testing and reporting
77 within each week. We then fit a generalized additive model [4] to the logged weekly
78 case estimates to obtain smooth trajectories for case time series. Finally, we take the
79 derivative of the predicted logged numbers of cases caused by each variant to obtain
80 time-varying growth rate estimates.

81 To obtain confidence intervals on the estimated time-varying growth rates, we
82 generate 1000 parameter sets by resampling spline coefficients from a multivariate
83 normal distribution using the estimated variance-covariance matrices. We calculate
84 time-varying growth rates from each parameter set and use equi-tailed quantiles to
85 generate 95% confidence limits.

86 **2.3 Estimating forward incubation-period distributions from 87 backward incubation-period distributions**

88 [3] estimated the incubation periods from 513 individuals (258 Omicron and 255 Delta
89 cases), with symptom onsets between 1 December 2021 and 2 January 2022. They
90 used the methods of [5], which estimates incubation period by inferring distributions
91 of time of infection for each individual from their known exposure dates, using a
92 uniform distribution, and compares this to a known symptom-onset time.

93 In practice, incubation periods (and other epidemiological delays) can be mea-
94 sured in two ways. The forward incubation periods are measured from a cohort of
95 individuals who were infected at the same time. We expect this forward incubation-
96 period distribution $f_I(\tau)$ to remain constant over the course of an epidemic and
97 provide reliable estimates of the distribution across individuals. Backward incuba-
98 tion periods are measured from a cohort of individuals who developed symptoms at
99 the same time. We expect the backward incubation-period distribution to be sensi-
100 tive to epidemic dynamics. The difference arises because forward incubation periods
101 look forward from the reference point towards symptom development, which is an

individual-level process, while backward incubation periods look backwards towards an infection event, which requires an interaction with an infectious individual.

In particular, when incidence of infection is growing exponentially, we are more likely to observe shorter backward incubation periods because there will be relatively more individuals who were infected recently. Specifically, the backward incubation-period distribution $b_I(\tau)$ corresponds to:

$$b_I(\tau) = \frac{\exp(-r\tau)f_I(\tau)}{\int_0^\infty \exp(-rx)f_I(x) dx}, \quad (1)$$

where r represents the epidemic growth rate. The method of [5] starts from observed symptom onsets, and estimates the backward incubation-period distribution without taking growth rates into account.

We adjust for observed growth rate of each variant by taking the backward incubation-period distributions estimated by [3] and calculating the corresponding forward incubation-period distributions by inverting Eq. (1):

$$f_I(\tau) = \frac{\exp(r\tau)b_I(\tau)}{\int_0^\infty \exp(rx)b_I(x) dx}. \quad (2)$$

We model the backward incubation-period distribution $b_I(\tau)$ using a Weibull distribution based on the assumptions of [3]. To account for uncertainties in the original parameter estimates, we rely on a sampling scheme, similar to the one we used for the growth rate analysis (in Section 2.2). First, we approximate the previously inferred posterior distributions of the shape and scale parameters of the Weibull distribution using a lognormal distribution—we parameterize the lognormal distribution such that (i) its median matches the median of the posterior distributions and (ii) the probability that a random variable following the specified Gamma distribution falls between the lower and upper credible limits matches 95% [6]. We draw 1000 samples of the shape and scale parameters (for the backward distribution $b_I(\tau)$) from the specified lognormal distributions and estimate the corresponding forward distribution using Eq. (2). We take 95% equi-tailed quantiles to obtain 95% confidence intervals.

2.4 Estimating forward generation-interval distributions from forward serial-interval distributions

Dynamical biases in the serial-interval distributions are more complex because the serial interval depends on the incubation periods of the infector and the infectee as well as the generation interval between them. For example, [3] measured the forward serial-interval distributions from cohorts of infectors who developed symptoms during the same week. In this case, the forward serial interval τ_s can be expressed in the form [2]:

$$\tau_s = -\tau_{i,1} + \tau_{g,\text{symp}} + \tau_{i,2}, \quad (3)$$

135 where $\tau_{i,1}$ represents the backward incubation period of the infector (because all
 136 infectors developed symptoms at the same time), and $\tau_{i,2}$, represents the forward
 137 incubation period of the infectee. Here, $\tau_{g,\text{symp}}$ represents the generation interval
 138 between the infector and the infectee; we use the subscript *symp* to indicate that
 139 these generation intervals are measured from infectors who developed symptoms at
 140 the same time.

The symptom-based generation-interval distribution describing Eq. (3) gives a bi-
 ased picture because infectors who developed symptoms at the same time will have
 shorter incubation periods (when epidemic is growing) and therefore transmit ear-
 lier. This symptom-based generation-interval distribution depends on the backward
 incubation-period distribution:

$$f_{G,\text{symp}}(\tau) = \int_0^\infty f_{G|I}(\tau|x)b_I(x) dx, \quad (4)$$

where $f_{G|I}(\tau|x)$ represents the forward generation-interval distribution conditional on
 a known value of the incubation period, x . Instead, the forward generation-interval
 distribution measured from a cohort of individuals who were infected at the time is
 expected to provide reliable estimates of the distribution across individuals (because
 their incubation-period distribution is expected to remain constant over time):

$$f_{G,\text{inf}}(\tau) = \int_0^\infty f_{G|I}(\tau|x)f_I(x) dx. \quad (5)$$

141 When epidemic is growing is exponentially, we have two opposing effects affecting
 142 the relationship between the mean serial and generation interval. First, infectors in
 143 a given cohort are more likely to have shorter incubation periods than their infectees
 144 on average, $\mathbb{E}[\tau_{i,1}] < \mathbb{E}[\tau_{i,2}]$, causing the mean forward serial interval to be longer
 145 than the mean symptom-based generation interval ($\mathbb{E}[\tau_s] > \mathbb{E}[\tau_{g,\text{symp}}]$). Second, the
 146 mean symptom-based generation interval will be shorter than the mean infection-
 147 based generation interval: $\mathbb{E}[\tau_{g,\text{inf}}] > \mathbb{E}[\tau_{g,\text{symp}}]$. Therefore, the difference between the
 148 mean serial interval and the mean infection-based generation interval is difficult to
 149 predict in general; in most cases, however, we expect the former effect to dominate,
 150 causing the mean serial interval to be longer than the mean infection-based generation
 151 interval: $\mathbb{E}[\tau_s] > \mathbb{E}[\tau_{g,\text{inf}}]$ [2]. For simplicity, we will use the term “forward generation-
 152 interval” to refer to the infection-based generation-interval distribution (measured
 153 from a cohort of infectors who were infected at the same infection time), and drop
 154 the subscript *inf*.

155 We model the forward incubation-period $f_I(\tau)$ and generation-interval $f_G(\tau)$ dis-
 156 tributions using a bivariate lognormal distribution. The joint distribution is parame-
 157 terized by log means, μ_I and μ_G , log variances, σ_I^2 and σ_G^2 , and the correlation coeffi-
 158 cient on a log scale ρ . Thus, the forward generation-interval distribution conditional
 159 on the incubation period $f_{G|I}(\tau|\tau_{i,1})$ has a log mean of $\mu_G + \sigma_G\rho(\log(\tau_{i,1}) - \mu_I)/\sigma_I$
 160 and a log variance of $\sigma_G^2(1 - \rho^2)$. Assuming that the incidence of infection is changing
 161 exponentially at rate r , the forward serial-interval distribution $f_S(\tau)$ for a cohort of

162 infectors who developed symptoms at time $t = 0$ can be calculated by integrating
 163 across infection time of the infector $\alpha_1 < 0$ and of the infectee $\alpha_2 > \alpha_1$ [2]:

$$f_S(\tau) = \frac{1}{\phi} \int_{-\infty}^0 \int_{\alpha_1}^{\tau} \exp(r\alpha_1) f_{G|I}(\alpha_2 - \alpha_1 | -\alpha_1) f_I(-\alpha_1) f_I(\tau - \alpha_2) d\alpha_2 d\alpha_1, \quad (6)$$

164 where ϕ is a normalization constant chosen so that $\int f_S(x) dx = 1$; $-\alpha_1$ corresponds
 165 to the incubation period of the infector; $\alpha_2 - \alpha_1$ corresponds to the generation interval;
 166 and $\tau - \alpha_2$ corresponds to the incubation period of the infectee.

167 For a given value of r , we first estimate the forward incubation-period distri-
 168 bution from the backward distribution, previously estimated by [3], using Eq. (2).
 169 We then approximate the forward incubation-period distribution with a lognormal
 170 distribution by matching the mean and standard deviation. Using this incubation-
 171 period distribution, we fit Eq. (6) to the observed serial-interval data by minimizing
 172 the negative log-likelihood. We then calculate the mean forward generation interval
 173 using Eq. (5) and approximate the 95% confidence interval using the Delta method.
 174 We assume $\rho = 0.75$ throughout based on [7]—since we do not have individual-level
 175 data on infection and symptom onset times, we expect this parameter to be uniden-
 176 tifiable in practice. In Supplementary Material, we explore how assumptions about
 177 ρ affect inferences of the generation-interval distribution.

178 2.5 Estimating instantaneous reproduction number

179 We use our estimates of the generation-interval distributions to infer instantaneous
 180 reproduction numbers $\mathcal{R}(t)$ of the Delta and Omicron variant, as well as the ra-
 181 tio between two reproduction numbers. Estimating the instantaneous reproduction
 182 number—defined as the average number of secondary infections that a primary case
 183 will generate if epidemiological conditions remain constant [8]—requires the intrinsic
 184 generation-interval distribution $g(\tau)$:

$$\mathcal{R}(t) = \frac{i(t)}{\int_0^\infty i(t-x)g(x) dx}, \quad (7)$$

185 where $i(t)$ represents incidence of infection. Here, we approximate the intrinsic
 186 generation-interval distribution with the forward generation-interval that we esti-
 187 mate for week 50—when epidemic is growing or decaying exponentially, we expect the
 188 forward generation-interval to be a good proxy for the intrinsic generation-interval
 189 distribution [9, 10]. Incidence of infection is approximated by shifting the smoothed
 190 case trajectories by one week to account for reporting delays. This method of ap-
 191 proximating incidence of infection assumes a fixed delay between infection and case
 192 reporting; in practice, deconvolution is required to accurately estimate the incidence
 193 of infection [11]. Case reports are also sensitive to changes in testing behavior, and
 194 therefore our estimates of $\mathcal{R}(t)$ must be interpreted with care. Confidence inter-
 195 vals are calculated by sampling parameters of the smoothed case trajectories as well
 196 as the generation-interval distributions from multivariate normal distributions and
 197 repeating the analysis 1000 times.

3 Results

Fig. 1 summarizes the epidemiological context in the Netherlands during the study period. The first known Omicron case in the Netherlands was sampled on 19 November 2021 [3], during a period when COVID-19 incidence was decreasing (Fig. 1A). As the Omicron variant continued to spread and increase in proportion (Fig. 1B), the number of COVID-19 cases started to increase (Fig. 1A). Multiplying the proportion of each variant with the number of reported COVID-19 cases further allows us to estimate the epidemiological dynamics of each (Fig. 1C). The number of COVID-19 cases caused by the Delta variant continued to decrease throughout the study period with time-varying growth rates decreasing from $r \approx -0.01/\text{day}$ to $r \approx -0.09/\text{day}$ by the week of January 16, 2022, and increasing back up to $r \approx -0.04/\text{day}$. The number of COVID-19 cases caused by the Omicron variant increased rapidly but decelerated over time with time-varying growth rates decreasing from $r = 0.18/\text{day}$ on the week of December 19, 2021, to $r = 0.04/\text{day}$. Finally, we find that the growth-rate difference between the Delta and Omicron variants decreased over time.

For a cohort of individuals who developed symptoms between 1 December 2021 and 2 January 2022, [3] found longer mean (backward) incubation period for the Delta variant than for the Omicron variant (Fig. 2A). However, these measurements were done during a period when the incidence of Omicron was increasing while the increasing of Delta was decreasing (Fig. 1). Thus, dynamical bias would be expected to lead to shorter observed (backward) incubation periods in Omicron, and longer observed incubation periods in Delta. When we account for these growth-rate differences and re-estimate the forward incubation periods, we find that both variants have similar incubation-period distributions (Fig. 2B)—for illustrative purposes, we assume $r = -0.05/\text{day}$ and $r = 0.15/\text{day}$ for the Delta and Omicron variants, respectively. Although the exact estimate of the mean forward incubation periods of both variants are sensitive to the assumed growth/decay rates, we find similar means across a plausible ranges of growth rates with unclear differences between two variants (Fig. 2C). For example, the mean forward incubation period of the Delta variant changes from 3.8 days (95% CI: 3.5–4.1 days) to 4.4 days (95% CI: 4.0–4.8 days) as we change the assumed values of r from $-0.1/\text{days}$ to $0/\text{days}$, while the mean forward incubation period of the Omicron variant changes from 3.8 days (95% CI: 3.4–4.4 days) to 4.5 days (95% CI: 3.9–5.5 days) as we change the assumed values of r from $0.1/\text{days}$ to $0.2/\text{days}$.

Our corrected estimates of the forward incubation-period distributions further allow us to infer the forward generation-interval distributions. For illustrative purposes, we first focus on within-household serial intervals from infectors who developed symptoms during week 50 (13–19 December, 2021)—[3] reported shorter mean serial interval of the Omicron variant (3.5 days) than that of the Delta variant (4.1 days) for this cohort (Fig. 3A). When we account for growth-rate differences (assuming $r = -0.05/\text{day}$ and $r = 0.15/\text{day}$ for the Delta and Omicron variants, respectively), the estimated mean forward generation interval exhibits a larger difference (Fig. 3B):

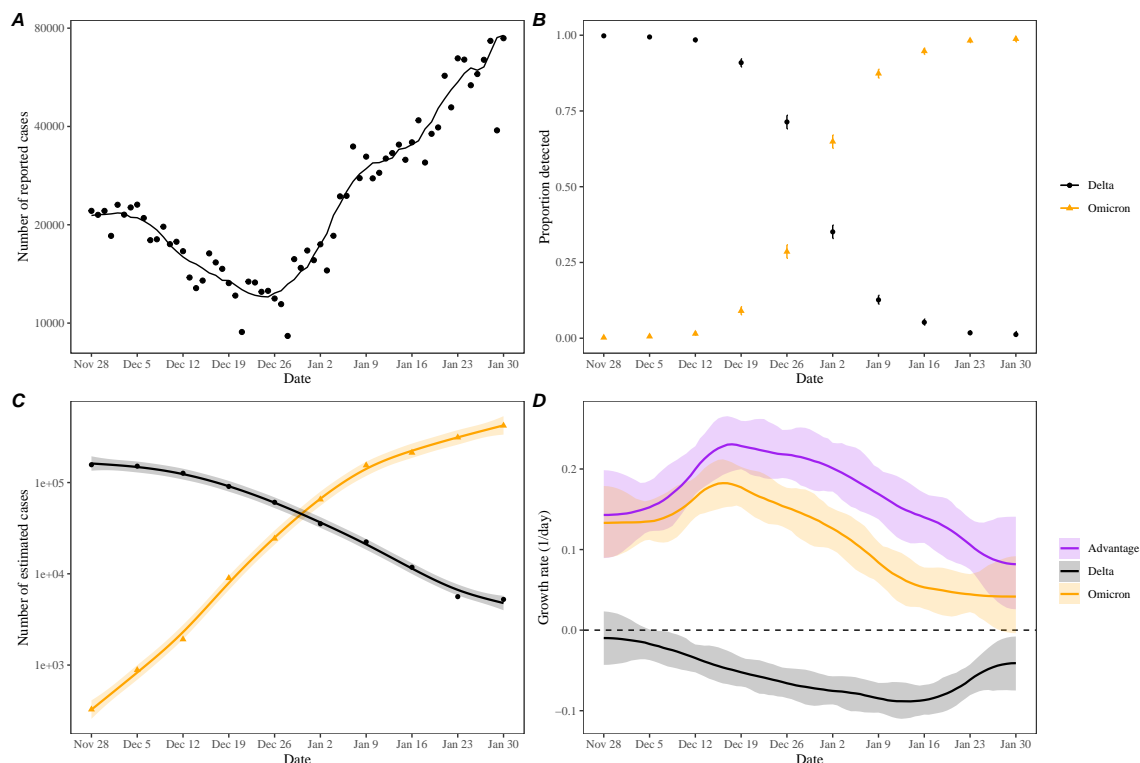


Figure 1: **Epidemic dynamics on the Delta and Omicron variants in the Netherlands.** (A) Daily numbers of reported COVID-19 cases in the Netherlands (points). The solid line represents the 7-day moving average. Data are publicly available on <https://data.rivm.nl/covid-19/>. (B) Proportion of SARS-CoV-2 variants detected from the Netherlands. Data are publicly available on <https://www.rivm.nl/coronavirus-covid-19/virus/varianten>. (C) Weekly numbers of COVID-19 cases caused by the Delta (black points) and Omicron (orange triangles) variants are estimated by multiplying the weekly numbers of cases (A) with the proportion of each variant (B). Solid lines and shaded areas represent fitted lines and corresponding 95% confidence intervals using generalized additive model. (D) Estimated growth rates of the Delta (black) and Omicron variants (orange) and their growth-rate differences (purple). Lines and shaded areas represent medians and corresponding 95% confidence intervals. Growth rates are estimated by taking the derivative of the generalized additive model estimates.

240 3.3 days (95% CI: 2.8–3.7 days) for the Omicron variant and 4.2 days (95% CI: 4.0–4.4
 241 days). Notably, both variants have similar mode, but the transmissibility of the omi-
 242 cron variant is estimated to decay much faster (Fig. 3B). Note that the mean forward
 243 generation interval of the Omicron (respectively, Delta) variant is shorter (longer)
 244 than its mean serial interval due to the effect of a growing (declining) epidemic.
 245 The estimated differences of the mean generation interval increase if we assume that
 246 generation intervals and incubation periods are less correlated (and therefore, lower

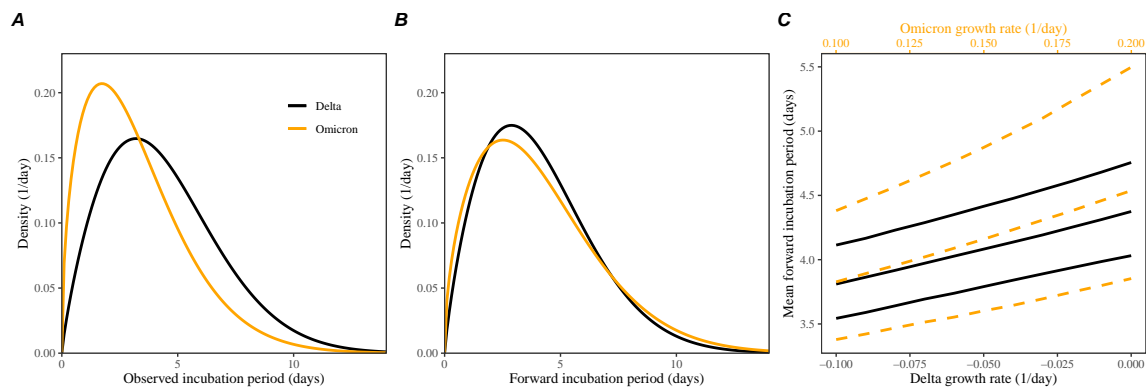


Figure 2: Observed and corrected differences in incubation-period distributions of Delta and Omicron variants. (A) Posterior median estimates of the observed (backward) incubation periods of the Delta (black) and Omicron (orange) variants by [3]. (B) Forward incubation-period distributions assuming $r = -0.05/\text{day}$ and $r = 0.15/\text{day}$ for the Delta (black) and Omicron (orange) variants, respectively. (C) Corrected estimates of the forward incubation-period distributions for different assumptions about the growth rates of the Delta (black, solid lines) and Omicron variants (orange, dashed lines). Middle lines represent median estimates, and lower and upper lines represent corresponding 95% confidence intervals.

values of ρ ; Supplementary Figure S1). On the other hand, neglecting growth-rate differences (i.e., assuming $r = 0/\text{day}$ for both variants) leads to the underestimation of these differences (Supplementary Figure S2): 3.5 days (95% CI: 3.1–3.9 days) for the Omicron variant and 4.1 days (95% CI: 3.9–4.3 days).

We then estimate the mean forward generation intervals for all other cohorts, stratified by the week of symptom onset (weeks 50 and 51) and the type of transmission (within and between household(s)). As before (see Fig. 2C), we repeat the analysis for different values of growth rates for the Delta ($r = -0.1/\text{days}$ to $0/\text{days}$) and Omicron ($r = 0.1/\text{days}$ to $0.2/\text{days}$) variants and plot the maximum likelihood estimates and the associated CIs. We estimate shorter mean forward generation intervals for the Omicron variant across all stratification (Fig. 3C), but the differences in the mean generation intervals are unclear for between-household pairs. Consistent with the original study, which also reported shorter mean forward serial intervals for between-household pairs [3], we estimate shorter mean forward generation intervals for between-household pairs. We also estimate a reduction in the mean forward generation intervals from week 50 to week 51.

Accounting for differences in the generation-interval distributions, we estimate that the reproduction number of the Omicron variant decreased from 1.83 (95% CI: 1.65–2.05) to 1.17 (95% CI: 1.00–1.36) between December 12, 2021, and January 23, 2022 (Fig. 4A). On the other hand, the reproduction number of the Delta variant decreased from 0.89 (95% CI: 0.82–0.97) to 0.68 (95% CI: 0.62–0.74) between December 5, 2021, and January 9, 2022, and increased back up to 0.82 (95% CI: 0.72–0.93)

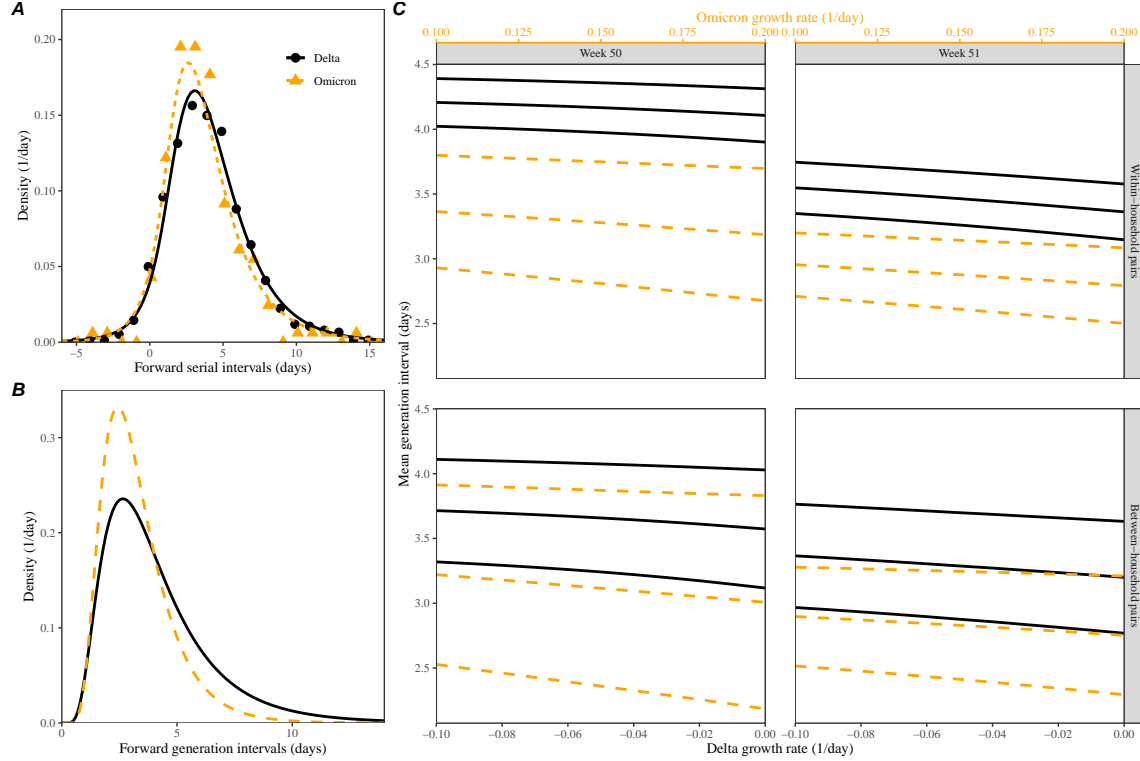


Figure 3: Estimated forward generation-interval distributions of Delta and Omicron variants. (A) Observed and fitted forward serial-interval distributions for within-household transmission pairs in the Netherlands for the Delta (black) and Omicron (orange) variants [3]. Serial intervals are calculated for infectors who developed symptoms on week 50 (13 and 19 December, 2021). Points represent the observed data. Lines represent the fitted lines assuming $r = -0.05/\text{day}$ for the Delta variant and $r = 0.15/\text{day}$ for the Omicron variant. Bivariate lognormal distributions with correlation coefficient of 0.75 are used to model relationships between incubation and generation intervals. (B) Estimated forward generation-interval distributions for within-household transmission pairs in the Netherlands. (C) Sensitivity of the mean generation-interval estimates to assumed growth rates of the Delta (black, solid lines) and Omicron variants (orange, dashed lines) stratified by the week of infectors' symptom onset and the type of transmission pairs.

by January 23, 2022 (Fig. 4A). We estimate the reproduction number ratios stayed roughly constant at around 2.2 (95% CI: 2.0–2.5) between December 12–26, 2021, and slowly decreased to 1.4 (95% CI: 1.2–1.7). However, if we neglect differences in the generation-interval distributions and solely rely on the generation-interval-distribution estimate for the Delta variant, we over-estimate the reproduction number of the Omicron variant and therefore is transmission advantage (Fig. 4B). In this case, the reproduction ratio decreases from 2.5 (95% CI: 2.2–2.8) to 1.5 (95% CI: 1.2–1.8), corresponding to roughly 7–13% bias.

277 In both cases, the decrease in the reproduction number ratio coincides with the
 278 decrease in the reproduction number of the Omicron variant, implying that epidemi-
 279 ological changes driving the dynamic had larger effects on the transmission of the
 280 Omicron variant than on the transmission of Delta variant; a larger reduction in the
 281 reproduction number of the Omicron variant also caused its growth rate to decrease
 282 faster, causing changes in the growth-rate difference (Fig. 1D).

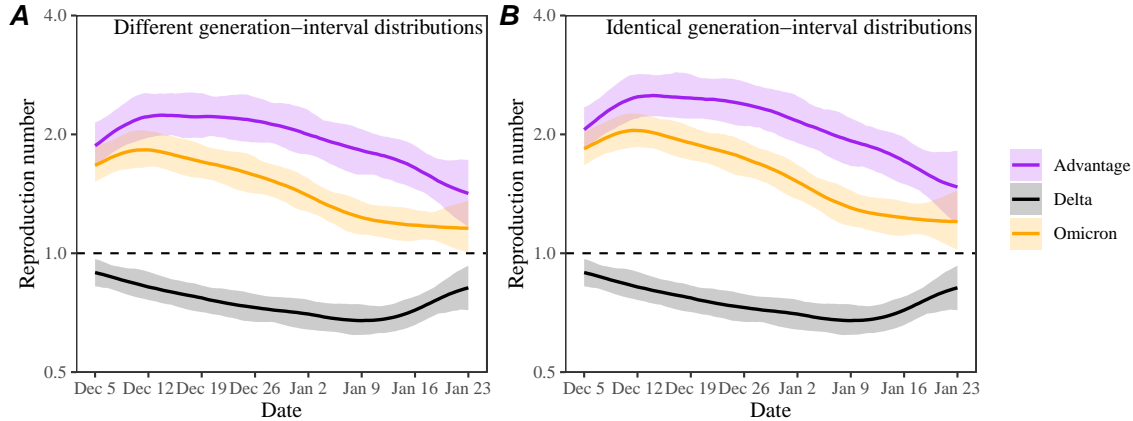


Figure 4: **Estimated time-varying reproduction number advantages of the Omicron variant.** (A) Estimated instantaneous reproduction numbers and their ratios over time while accounting for differences in the generation-interval distributions. (B) Estimated instantaneous reproduction numbers and their ratios over time while assuming identical generation-interval distributions. The instantaneous reproduction number of each variant is estimated using the renewal equation by shifting the smoothed case curves by one week (Fig. 1C). The intrinsic generation-interval distribution is approximated by the maximum likelihood estimates of the generation-interval distributions for within-household transmission pairs based on $r = -0.05$ for the Delta variant (black) and $r = 0.15$ for the Omicron variant (orange). Purple lines represent the ratio between the effective reproduction numbers of the Delta and Omicron variants. Lines and shaded regions represent medians and corresponding 95% confidence intervals.

283 4 Discussion

284 We compare estimates of the forward incubation-period and generation-interval dis-
 285 tributions of the Delta and Omicron variants from the Netherlands. The original
 286 analysis detailing the data set previously reported shorter mean incubation period
 287 and serial interval for the Omicron variant [3]. Accounting for differences in epi-
 288 demic growth rates, we find similar incubation-period distributions for both variants
 289 but a considerably shorter (0.5–0.9 days) mean generation interval for the Omicron
 290 variant. The mean forward generation interval of both variants further decreased

291 between week 50 (13–19 December, 2021) and week 51 (20–26 December, 2021). Fi-
 292 nally, we estimate that the transmission advantage of the Omicron variant decreased
 293 from 2.2-fold to 1.4-fold between early December and late January. Neglecting dif-
 294 ferences in the generation-interval distributions can result in $\approx 10\%$ bias in estimates
 295 of the transmission advantage.

296 The generation-interval distribution describes changes in the individual-level trans-
 297 mission dynamics over the course of infection and therefore provides crucial infor-
 298 mation for epidemic control. A few studies have estimated the generation-interval
 299 distributions of SARS-CoV-2 infections from serial-interval data, but most of them
 300 neglect the effects of epidemic growth rates [12, 13, 14, 15]—these practices can be
 301 largely attributed to historical work that concluded that serial and generation in-
 302 tervals have the same means based on the assumption that infectors and infectees
 303 have identical incubation-period distributions [16, 17, 18]. Here, we build on our
 304 previous work [2], which demonstrated theoretically that forward serial-interval dis-
 305 tributions depends on epidemic growth rates, and further confirm that estimates of
 306 the forward generation-interval distributions are indeed sensitive to epidemic growth
 307 rates. Accounting for the growth-rate effects is especially important when compar-
 308 ing serial and generation intervals of different variants or from different time periods.
 309 These effects are also pertinent to all epidemiological inferences of past events from
 310 a cohort of infected individuals who experienced the succeeding event at the same
 311 time—this includes inferences of other delay distributions, such as incubation-period
 312 distributions, as well as viral load trajectories [19].

313 To our knowledge, our study is the first to estimate the generation-interval dis-
 314 tribution of the Omicron variant. Although we estimate a shorter mean generation
 315 interval for the Omicron variant, we find the generation-interval distribution of the
 316 Omicron and Delta variants have similar modes (around 2.5 days), implying that
 317 the realized transmissibility of the Omicron variant decays faster. We tentatively
 318 hypothesize that these differences may be primarily driven by the network effect: a
 319 higher reproduction numbers of the Omicron variant leads to faster susceptible de-
 320 pletion among close contacts, which in turn prevents long generation intervals from
 321 generating infections [10, 15]. While the network effect is expected to be strongest
 322 among household contacts, it is also applicable to other forms of contact structures
 323 that involve repeated contacts between the same group of individuals (because only
 324 the first infectious contact results in infection). The network effect may also explain a
 325 decrease in the mean generation interval between week 50 and 51, especially among
 326 household transmission pairs, as a higher proportion of individuals within house-
 327 holds would have been infected with either the Delta or Omicron variants. Other
 328 factors, such as more stringent intervention measures against the Omicron variant
 329 [3] and shorter clearance phase of the Omicron variant [20], also likely contributed
 330 to shortening of the generation intervals.

331 While our study indicate that the Omicron variant has a shorter mean realized
 332 generation interval than that of the Delta variant, it is still uncertain how much their
 333 infectiousness profiles differ intrinsically. In particular, similarities in the incubation-

334 period distributions of the Delta and Omicron variants suggest that the differences
 335 in their intrinsic infectiousness profile may be smaller than the estimated differences
 336 in their realized generation-interval distributions. Nonetheless, our estimates of the
 337 realized generation-interval distributions better describe the epidemic dynamics, im-
 338 plicitly accounting for intervention and behavioral effects, and are therefore should
 339 be used to estimate current reproduction numbers (rather than a counterfactual
 340 intrinsic generation-interval distribution, which may have a longer mean).

341 Our study also has important implications for estimating transmission advantages
 342 of new SARS-CoV-2 variants. In the example we consider, neglecting differences in
 343 the generation-interval distributions leads to $\approx 10\%$ bias in the estimates of the re-
 344 production number ratios; however, the degree of ratio is expected to be sensitive
 345 to the assumed generation-interval distribution of the resident variant. For example,
 346 [21] estimated a much higher reproduction ratios (> 4 fold) in South Africa but also
 347 assumed a longer mean generation interval for the Delta and Omicron variants (6.4 vs
 348 5.2 days, respectively). With our generation-interval estimates, we estimate that the
 349 reproduction number ratio of 2.8 assuming $r = -0.06$ and $r = 0.26$ for the Delta and
 350 Omicron variants, respectively—these growth rates were chosen to match the 4-fold
 351 reproduction number ratios with the estimated growth-rate differences of 0.32/day
 352 for the Gauteng province, South Africa [21]. We also show that both growth-rate dif-
 353 ferences and the reproduction number ratios decreased over time—this result further
 354 corroborates are earlier theoretical framework, which showed that growth-rate dif-
 355 ferences changes over the course of an epidemic even when the reproduction number
 356 ratios remain constant [22].

357 We primarily rely on case data to understand epidemic patterns of the Delta and
 358 Omicron variants. In doing so, we implicitly assume that the delay between infection
 359 and reports is fixed. However, changes in case trajectories are sensitive to testing
 360 patterns and therefore may not accurately reflect patterns of infections. While this
 361 limitation does not affect our generation-interval estimates, our inferences of the
 362 transmission advantages of the Omicron variant should be interpreted with care.

363 Monitoring changes in key epidemiological parameters is critical to understanding
 364 the evolution of SARS-CoV-2 and predicting its future dynamics [23]. Our study syn-
 365 thesises previously developed theoretical framework on serial- and generation-interval
 366 distributions and presents methodological advances in monitoring epidemiological
 367 parameters; however, uncertainty remains in the intrinsic infectiousness profiles of
 368 SARS-CoV-2 variants, especially among asymptotically infected individuals [24].
 369 Future studies extending our framework and combining more detailed epidemiologi-
 370 cal data will be critical to narrowing down these uncertainties.

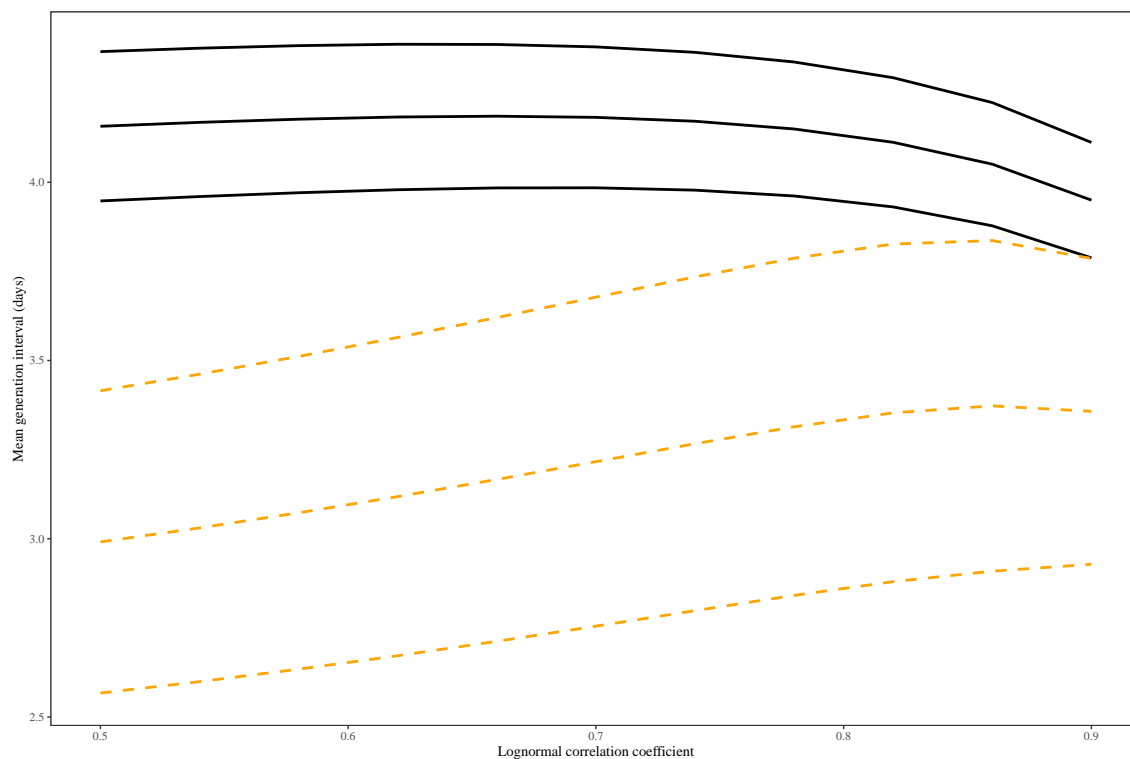


Figure S1: **Sensitivity of the estimates of the mean generation interval to the assumed values of the correlation coefficient of the lognormal distribution.** Lines represent maximum likelihood estimates and the corresponding 95% confidence intervals for the Delta (black, solid lines) and Omicron variants (orange, dashed lines). For illustrative purposes we use within-household serial-interval data from the cohort of infectors who developed symptoms during week 50.

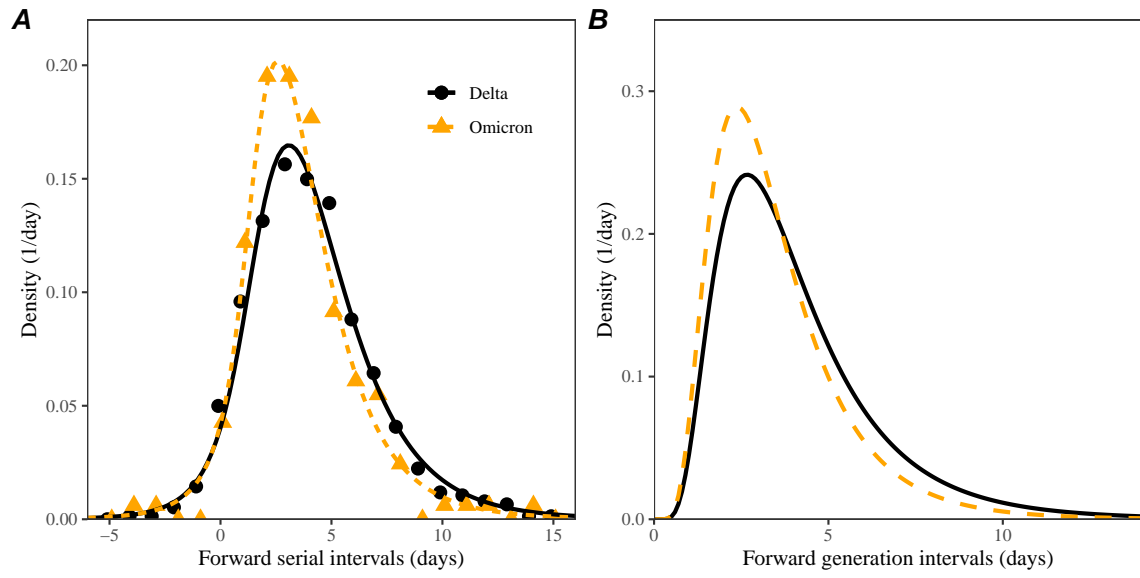


Figure S2: **Estimated forward generation-interval distributions of Delta and Omicron variants while neglecting growth-rate differences.** See Figure 3 in the main text for figure caption.

References

- [1] Sam Abbott, Katharine Sherratt, Moritz Gerstung, and Sebastian Funk. Estimation of the test to test distribution as a proxy for generation interval distribution for the Omicron variant in England. *medRxiv*, 2022.
- [2] Sang Woo Park, Kaiyuan Sun, David Champredon, Michael Li, Benjamin M Bolker, David JD Earn, Joshua S Weitz, Bryan T Grenfell, and Jonathan Dushoff. Forward-looking serial intervals correctly link epidemic growth to reproduction numbers. *Proceedings of the National Academy of Sciences*, 118(2), 2021.
- [3] Jantien A Backer, Dirk Eggink, Stijn P Andeweg, Irene K Veldhuijzen, Noortje van Maarseveen, Klaas Vermaas, Boris Vlaemynck, Raf Schepers, Susan van den Hof, Chantal BEM Reusken, and Jacco Wallinga. Shorter serial intervals in SARS-CoV-2 cases with Omicron BA.1 variant compared with Delta variant, the Netherlands, 13 to 26 December 2021. *Eurosurveillance*, 27(6):2200042, 2022.
- [4] Simon N Wood. mgcv: GAMs and generalized ridge regression for R. *R News*, 1(2):20–25, 2001.
- [5] Jantien A Backer, Don Klinkenberg, and Jacco Wallinga. Incubation period of 2019 novel coronavirus (2019-nCoV) infections among travellers from Wuhan, China, 20–28 January 2020. *Eurosurveillance*, 25(5):2000062, 2020.
- [6] Sang Woo Park, Benjamin M Bolker, David Champredon, David JD Earn, Michael Li, Joshua S Weitz, Bryan T Grenfell, and Jonathan Dushoff. Reconciling early-outbreak estimates of the basic reproductive number and its uncertainty: framework and applications to the novel coronavirus (SARS-CoV-2) outbreak. *Journal of the Royal Society Interface*, 17(168):20200144, 2020.
- [7] Ron Sender, Yinon M Bar-On, Sang Woo Park, Elad Noor, Jonathan Dushoffd, and Ron Milo. The unmitigated profile of COVID-19 infectiousness. *medRxiv*, 2021.
- [8] Christophe Fraser. Estimating individual and household reproduction numbers in an emerging epidemic. *PloS one*, 2(8):e758, 2007.
- [9] David Champredon and Jonathan Dushoff. Intrinsic and realized generation intervals in infectious-disease transmission. *Proceedings of the Royal Society B: Biological Sciences*, 282(1821):20152026, 2015.
- [10] Sang Woo Park, David Champredon, and Jonathan Dushoff. Inferring generation-interval distributions from contact-tracing data. *Journal of the Royal Society Interface*, 17(167):20190719, 2020.

- [11] Edward Goldstein, Jonathan Dushoff, Junling Ma, Joshua B Plotkin, David JD Earn, and Marc Lipsitch. Reconstructing influenza incidence by deconvolution of daily mortality time series. *Proceedings of the National Academy of Sciences*, 106(51):21825–21829, 2009.
- [12] Tapiwa Ganyani, Cecile Kremer, Dongxuan Chen, Andrea Torneri, Christel Faes, Jacco Wallinga, and Niel Hens. Estimating the generation interval for coronavirus disease (COVID-19) based on symptom onset data, March 2020. *Eurosurveillance*, 25(17):2000257, 2020.
- [13] Xi He, Eric HY Lau, Peng Wu, Xilong Deng, Jian Wang, Xinxin Hao, Yiu Chung Lau, Jessica Y Wong, Yujuan Guan, Xinghua Tan, et al. Temporal dynamics in viral shedding and transmissibility of COVID-19. *Nature medicine*, 26(5):672–675, 2020.
- [14] Shi Zhao, Biao Tang, Salihu S Musa, Shujuan Ma, Jiayue Zhang, Minyan Zeng, Qingping Yun, Wei Guo, Yixiang Zheng, Zuyao Yang, et al. Estimating the generation interval and inferring the latent period of COVID-19 from the contact tracing data. *Epidemics*, 36:100482, 2021.
- [15] William S Hart, Elizabeth Miller, Nick J Andrews, Pauline Waight, Philip K Maini, Sebastian Funk, and Robin N Thompson. Generation time of the alpha and delta SARS-CoV-2 variants: an epidemiological analysis. *The Lancet Infectious Diseases*, 2022.
- [16] Åke Svensson. A note on generation times in epidemic models. *Mathematical biosciences*, 208(1):300–311, 2007.
- [17] Tom Britton and Gianpaolo Scalia Tomba. Estimation in emerging epidemics: biases and remedies. *Journal of the Royal Society Interface*, 16(150):20180670, 2019.
- [18] Sonja Lehtinen, Peter Ashcroft, and Sebastian Bonhoeffer. On the relationship between serial interval, infectiousness profile and generation time. *Journal of the Royal Society Interface*, 18(174):20200756, 2021.
- [19] James A Hay, Lee Kennedy-Shaffer, Sanjat Kanjilal, Niall J Lennon, Stacey B Gabriel, Marc Lipsitch, and Michael J Mina. Estimating epidemiologic dynamics from cross-sectional viral load distributions. *Science*, 373(6552):eabh0635, 2021.
- [20] James A Hay, Stephen M Kissler, Joseph R Fauver, Christina Mack, Caroline G Tai, Radhika M Samant, Sarah Connelly, Deverick J Anderson, Gaurav Khullar, Matthew MacKay, et al. Viral dynamics and duration of PCR positivity of the SARS-CoV-2 Omicron variant. *medRxiv*, 2022.

- 443 [21] Carl AB Pearson, Sheetal P Silal, Michael WZ Li, Jonathan Dushoff, Ben-
 444 jamin M Bolker, Sam Abbott, Cari van Schalkwyk, Nicholas G Davies,
 445 Rosanna C Barnard, W John Edmunds, et al. Bounding the levels of trans-
 446 missibility & immune evasion of the Omicron variant in South Africa. *MedRxiv*,
 447 2021.
- 448 [22] Sang Woo Park, Benjamin M Bolker, Sebastian Funk, C Jessica E Metcalf,
 449 Joshua S Weitz, Bryan T Grenfell, and Jonathan Dushoff. Roles of generation-
 450 interval distributions in shaping relative epidemic strength, speed, and control
 451 of new SARS-CoV-2 variants. *medRxiv*, 2021.
- 452 [23] Moritz UG Kraemer, Oliver G Pybus, Christophe Fraser, Simon Cauchemez,
 453 Andrew Rambaut, and Benjamin J Cowling. Monitoring key epidemiological
 454 parameters of SARS-CoV-2 transmission. *Nature medicine*, 27(11):1854–1855,
 455 2021.
- 456 [24] Sang Woo Park, Daniel M Cornforth, Jonathan Dushoff, and Joshua S Weitz.
 457 The time scale of asymptomatic transmission affects estimates of epidemic po-
 458 tential in the COVID-19 outbreak. *Epidemics*, 31:100392, 2020.